A new Unidentified Far Infrared Band in NGC 7027

Javier R. Goicoechea, José Cernicharo, Helena Masso and María Luisa Senent

Departamento de Astrofísica Molecular e Infrarroja, Instituto de Estructura de la Materia, CSIC, Serrano 121, E–28006 Madrid, Spain.

javier@damir.iem.csic.es, cerni@damir.iem.csic.es, masso@damir.iem.csic.es, imts420@iem.cfmac.csic.es

ABSTRACT

We report on the detection of a molecular band centered at ∼98 μm (∼102 cm^{-1}), observed with the *Infrared Space Observatory*[1] in the young Planetary Nebula NGC 7027. The band structure and intensity can not be reproduced by atomic fine structure lines, recombination lines or by the rotational emission of abundant molecules. We discuss the possible contribution of the low–energy bending modes of pure carbon chains to the unidentified far–IR bands observed in *C*–rich evolved objects. In particular, we speculate that the band emission could arise from the ν_9 and ν_7 bending modes of C_6 and C_5, for which wavenumbers of 90±50 and 107±5 cm^{-1} have been estimated from photoelectron spectroscopy.

Subject headings: infrared: stars — circumstellar matter — stars: individual (NGC 7027) — ISM: molecules — line: identification

1. Introduction

Carbon chains molecules are of special interest for Astrophysics since Douglas (1977) proposed them as possible carriers of the diffuse interstellar bands (DIBs). In the past years, many polar carbon chains have been detected in the interstellar and circumstellar media (ISM and CSM) through their pure rotational spectrum at radio wavelengths. Major examples are the cyanopolyynes, $HC_{2n+1}N$ with n=1–5 (Turner 1971, Avery et al. 1976, Kroto et al. 1978, Broten et al. 1978, Bell et al. 1997), and the hydrogenated carbon chain

[1]Based on observations with ISO, an ESA project with instruments funded by ESA Member States (especially the PI countries: France, Germany, the Netherlands and the United Kingdom) and with participation of ISAS and NASA.

radicals such as C_5H, C_6H, C_7H and C_8H (Cernicharo et al. 1986, Guélin et al. 1987, 1997, Cernicharo & Guélin 1996).

On the other hand, larger carbon molecular complexes such as the polyatomic aromatic hydrocarbons (PAHs) are believed to dominate the ubiquitous mid–IR emission seen in the unidentified infrared bands (UIBs). However, only the single aromatic species, benzene, has been so far identified through its IR active modes (Cernicharo et al. 2001).

All this chemistry richness suggests that the growth mechanisms producing complex carbon molecules such as the PAHs or the fullerenes are highly efficient. Nevertheless, the set of 'building blocks" and the possible chemical reactions still have to be identified and clarified. Among the possible species, the pure carbon chains, (C_n; Van Orden & Saykally 1998), could be the 'skeletons" from which larger organic molecules can be formed (see Cernicharo, Goicoechea & Caux 2000, Cernicharo 2004). Due to the lack of permanent electric dipole, these species do not have rotational spectrum to be observed from radio telescopes. The only way to detect them in the dense ISM and CSM is through their asymmetrical stretching modes around $\sim$5 μm (2000 cm^{-1}) and/or through their low–energy bending modes around $\sim$100 μm ($\sim$100 cm^{-1}). The first technique allowed the detection of C_3 (Hinkle et al. 1988) and C_5 (Bernath et al. 1989) in the circumstellar envelope of the bright IR evolved star IRC+10216. However, few sources (specially in the ISM) have enough flux at $\sim$5 μm to allow systematic studies of the C_n stretching modes, and the less known far–IR bending modes are the only way to detect these species.

Before the launch of ISO (Kessler et al. 1996), we proposed to observe the bending modes of several polyatomic molecules in the far–IR. As a result, the ν_2 bending mode of C_3 has been observed in Sgr B2 and IRC+10216 (Cernicharo et al. 2000). In addition, we have detected several Unidentified far-IR bands (UfIBs) in the ISO spectrum of many C–rich sources that may also be related with the bending modes of carbon chains species. In particular we have tentatively assigned a UfIB at $\sim$57.5 μm ($\sim$174 cm^{-1}), observed in Sgr B2 and in *C*–rich evolved stars including the planetary nebula (PNe) NGC 7027, to the ν_5 bending mode of C_4 (Cernicharo, Goicoechea & Benilan 2002).

NGC 7027 is one of the most studied evolved objects in the Galaxy. It is a young PNe, $\sim$1000 years since it left the AGB stage, characterized by a relatively compact ionized region (Volk & Kwok 1997) driven by the radiation that arises from a central source at $\sim$200,000 K (Latter et al. 2000). In addition, a rich *C*–chemistry is taking place in the larger molecular envelope ($\sim$40$''$ in CO; Masson et al. 1985) that surrounds the inner photon dominated regions. In fact, NGC 7027 was the first object to show UIB emission latter attributed to the PAH emission (Gillett et al. 1973) and the only source where pure rotational lines of CH^+ have been detected (Cernicharo et al. 1997).

Therefore, the detection of unidentified features in the IR spectrum of NGC 7027 has historically contributed to a better understanding of the interstellar carbon complexity. In this work, we report the detection of a new UfIB at ∼98 μm (∼102 cm^{-1}) in the far–IR spectrum of NGC 7027 and speculate about it possible origin.

2. Observations

The possible emission/absorption produced by the low–energy bending modes of C_n species has been searched using the *Long–Wavelength Spectrometer* (LWS; Clegg et al. Swinyard et al. 1996). In the case of the NGC 7027 PNe, we have used all the LWS AOT L01 data taken by ISO (see Herpin et al. 2002). The LWS grating spectra of NGC 7027 taken during orbits 21, 342, 349, 356, 363, 377, 537, 552, 559, 566, 579, 587, 594, 601, 706, 713, 720, 727, 734, 741, 755, 762, 769, 776, and 783 have been averaged. The total on-source time was 53409 s and the signal–to–noise (S/N) ratio is very high. Here we present part of the spectrum taken with the LWS between ∼86 and 110 μm (∼116–91 cm^{-1}) at a resolution of $\lambda/\Delta\lambda \simeq 200$. The resulting spectrum is shown in Fig. 1, *middle panel*. We also present the same wavelength range in the LWS spectrum [TDT19800158] of IRC+10216 (see Fig. 1, *lower panel*). The full spectrum was shown and modeled by Cernicharo et al. 1996.

All data were processed following pipeline number 9 and analyzed using the ISO Spectral Analysis Package[2] (ISAP). Typical routines include: deglitching spikes due to cosmic rays, oversampling and averaging individual scans and removing baselines polynomials.

In addition, we present part of the *Short–Wavelength Spectrometer* (SWS; de Graauw et al. 1996) spectrum of NGC 7027 between ∼4–7 μm (∼2500-1430 cm^{-1}). The resolution of the SWS01 observation template in this interval is $\lambda/\Delta\lambda \simeq 1500$. Many carbon chains (polar and non-polar) possess prominent IR active stretching modes in this wavelength range. However, Fig. 2 shows that the bulk of the emission in NGC 7027 arises from narrow ionic and recombination lines from the inner H II region. Only the well–known UIB broad emission at ∼6.2 μm is detected. This band corresponds to the relaxation of excited vibrational states of aromatic species pumped by absorption of visible–UV photons from the hot central star. The full SWS spectrum has been presented by Bernard Salas et al. (2001).

---

[2]The ISO Spectral Analysis Package (ISAP) is a joint development by the LWS and SWS Instruments Teams and Data Centers. Contributing institutes are CESR, IAS, IPAC,MPE, RAL, and SRON.

3. Results

After identified and modeled the molecular rotational lines of CO J=30–29 to 25–24, CH^+ J=4–3 and OH $^2\Pi_{1/2}$ J=5/2–3/2 (see Herpin et al. 2002 for the details), a strong band–like feature constituted by several lines was identified between 91 and 102 μm. Only the high–J CO rotational emission produces modest contribution in the band wavelengths. Fig. 1 also shows the maximum contribution expected for the rotational $^2\Pi_{1/2}$ 5/2–3/2 line of OH at ∼98 μm estimated from the clearer detections at ∼79 and ∼84 μm. Note that no water lines have been detected in the far–IR spectrum of NGC 7027 (Cernicharo et al. 1997), and thus, no more O-bearing species are contaminating the ∼86–110 μm window.

Due to the presence of an H II region in the inner envelope, we have also searched for all the possible atomic transitions that could arise from the nebular gas. The most likely atomic lines in a PNe such as NGC 7027 (fine structure and recombination lines), taken from the *Atomic Line List* by Peter van Hoof have been analyzed. We note that lines from [V IV], [V III] and [Ti III], with transitions in the considered wavelength range, have been previously detected in the optical spectrum of NGC 7027 (Baluteau et al. 1995), while several H I recombination lines are observed in the mid–IR (e.g. see Fig. 2).

To estimate the H I emission in the far–IR we have considered a H II region ($2'' - 4''$) of ∼0.022 $M_\odot$(see the model of Volk & Kwok 1997) with n_H=n_e and assumed that the H I population is given by the Saha–Boltzmann equation. With these parameters, we can predict the H I recombination lines observed in the mid–IR by Bernard Salas et al. (2001), and estimate the opacity of the far–IR lines. We found that only the H$n\alpha$ series with n from 10 to 15 may produce modest emission in the LWS range. However, none of these lines appear between 90 and 110 μm. In addition, we have analyzed the possible overlapping with fine structure lines. In particular, the [Ti II]96.68, 106.27 and [V II]97.79 μm lines could produce some emission in the considered range. Even assuming a vanadium abundance 10 times larger than the solar abundance, the [V II]97.79 μm ($^5D_3$-$^5D_2$) line would be extremely weak. Note that the [V II]141.68 μm ($^5D_2$-$^5D_1$) line is neither detected in NGC 7027. Finally, the solar abundance of Ti is ∼10 times that of vanadium. We also computed that is too low to produce significant emission in the [Ti II]96.68, 106.27 lines.

Hence, the integrated band intensity and the different lines or sub-bands could not be fully assigned to any of these atomic lines nor to the pure rotational lines with significant line strength arising from the light species in the circumstellar envelope.

We also note that after subtracting the crowed emission of CO, HCN and HCN_{vib} (pure rotational lines in vibrational excited states) from the spectrum of IRC+10216, some of the remaining peaks also agreed with those unidentified peaks observed in NGC 7027 (see Fig.

1). However, the spectral resolution is too poor to distinguish unidentified features from the forest of HCN_{vib} rotational lines that contaminate the far–IR spectrum of IRC+10216 but are missing in NGC 7027. The HCN abundance in IRC+10216 is very high, $\sim 3\times10^5$, with HCN/CO=1/10. In fact, HCN is the main coolant of this *C*–rich AGB star (Cernicharo et al. 1999). However, the molecule is photodissociated during the post–AGB evolution as the UV radiation field from the evolving star increases. From far–IR observations of HCN pure rotational lines, Herpin et al. (2002) found minimum abundances of HCN/CO=1/100 and 1/1000 for the proto–PNe CRL 2688 and CRL 618 respectively. The extreme case is NGC 7027, were a great part of HCN molecules must have been photodissociatd in CN and H. In fact, Bachiller et al. (1997) found CN/HCN$\sim$10 for this object. Thus, the low abundance of HCN compared to IRC+10216 is consistent with the non detection of far–IR HCN lines (Herpin et al. 2002). Pure rotational lines of other cyanopolyynes species such as HC_3N can not produce emission in this range because of the high energy levels associated with its far–IR transitions.

Taking into account the high S/N ratio of the NGC 7027 spectrum, and the absence of the band in sources such as Orion, Sgr A or *O*–rich evolved stars, we believe that the lines are real. Due to the chemistry of NGC 7027, the most probable carrier should be the low–energy bending mode of a polyatomic molecule containing carbon.

4. Discussion

Both PAHs and pure carbon chains possesses low–energy bending modes in the far–IR. Contrary to the UIB emission in the mid–IR, the far–IR skeletal modes of PAHs (vibrations associated with the bending of the skeletal structure) depends of the exact nature of the species. Hence, the rovibrational structure of the PAH skeletal mode has to be calculated for each specific PAH. As a example, the lowest energy active mode of coronene ($C_{24}H_{12}$) lies at $\sim$127 cm^{-1} (Joblin et al. 2002), while for ovalene ($C_{32}H_{14}$), two far–IR skeletal modes at $\sim$120 cm^{-1} and $\sim$66 cm^{-1} have been theoretically investigated (Mulas et al. 2003). The far-IR emission of a few PAHs has also been observed in gas phase experiments (Zhang et al. 1996). However, if one of the observed UfIBs belongs to a specific PAHs, other bands (generally stronger) should be observed in the IR spectrum. This is not the case of the new UfIB presented in this work and we have considered the low–energy modes of pure carbon chains as possible carriers of the observed UfIB.

The detection of several rovibrational lines of the ν_2 bending mode of C_3 ($\sim$63 cm^{-1}) in Sgr B2 and IRC+10216 evidenced high abundances for this species and opened the possibility to detect more carbon chains in the ISM and CSM (Cernicharo et al. 2000). At the low

resolution of the LWS/grating, the more intense C_3 lines [Q(2,4,6)] are blended with the strong [C II]158 μm line and no assignation could be made in NGC 7027. However, the tentative detection of the ν_5 bending mode of C_4 in many objects including NGC 7027 ($\sim$174 cm^{-1}; Cernicharo et al. 2002), if confirmed, will imply a $C_3/C_4<10$ abundance ratio, which will suggest that the abundance of C_n does not decrease drastically when n increases.

In spite of their importance, the C_n bending modes are difficult to characterize spectroscopically in the laboratory or by *ab initio* computations. As expected, the main uncertainties difficulting their astronomical detection are the band origin and the IR intensity. Moreover, the induced dipole moments and other spectroscopic constants are often known for the fundamental transition but less or nothing is known about overtone transitions within the bending mode or transitions to other excited states including the stretching modes.

The ground electronic state is different for the odd– and even– numbered cumulenic chains. This property determines the observed band shape of the bending mode. Odd–numbered linear C_n's have a singlet $^1\Sigma_g^+$ ground electronic state which results in a perpendicular $^1\Pi_{vib} - {}^1\Sigma_{vib}$ vibronic spectrum with a strong $-Q$ branch and weak $-P$ and $-R$ branches. On the other hand, even–numbered linear C_n's have a triplet $^3\Sigma_g^-$ ground electronic state. Hence, each rotational line is split in three components due to spin couplings. This splitting increase with the number of atoms but is particularly small for C_4 and C_6 (Giesen et al. 2001). The vibronic transition is now $^3\Pi_{vib} - {}^3\Sigma_{vib}$, and despite the null component of the electronic orbital momentum in the ground state, the spin–orbit constant (A_{SO}) could be large in even– C_n's. In such a case, the resulting band–shape will be notoriously affected by the value of A_{SO}.

4.1. Tentative detection of C_6 and C_5

With the exception of the ν_2 mode of C_3, the band origins of other C_n bending modes are not accurately constrained. Hence, their assignation as carriers of the UfIBs is not obvious. Although the low–lying bending modes of C_5 and C_6 have not been directly observed in gas phase, different studies suggest wavenumbers around $\sim$100 cm^{-1} (see below). The observed new UfIB around $\sim$98 μm is composed by several peaks at $\sim$91.8, 92.8, 93.9, 95.2, 97.6, 98.9, 100.5 and 101.7 μm. In the following, we will consider the possibility that *any of these peaks is related with the ν_9 and ν_7 bending modes of C_6 and C_5 respectively.*

C_5 was first detected in the gas phase by Heath et al. (1989) who observed the ν_3 stretching mode at $\sim$2169 cm^{-1} ($\sim$4.6 μm). The same mode was observed in IRC+10216 by Bernath et al. (1989). Actually, C_5 is the largest C_n detected in the CSM. On the other hand,

C_6 was first identified in the laboratory by its electronic spin resonance spectrum in an Ar matrix (Van Zee et al. 1987) and later observed in gas phase through its ν_4 stretching mode at $\sim$1960 cm^{-1} ($\sim$5.1 μm) by Hwang et al. (1993). Moazzen–Ahmadi et al. (1989) observed the (ν_3+ν_7)–ν_7 and (ν_3+2ν_7)–2ν_7 hot bands arising from the ν_7 bending mode of C_5. From the l–doubling constant q_7, they estimated a frequency of ν_7=118$\pm$3 cm^{-1}. More recently, C_5 has been observed in photoelectron spectra. In particular, Arnold et al. (1991) measured the 2ν_7 transition and estimated ν_7=101$\pm$45 cm^{-1}, while Kitsopoulos et al. (1991) obtained ν_7=107$\pm$5 cm^{-1}. *Ab initio* calculations predict an infrared intensity around 36 km mol^{-1} [$A(\nu_7$=1-0)$\simeq$0.06 s^{-1}; Hutter & Lüthi 1994; Martin et al. 1995]. Fig. 1 shows the expected band–shape for a $^1\Pi_{vib} - {}^1\Sigma_{vib}$ transition with this intensity and the molecular constants for the ν_7 mode (Moazzen–Ahmadi et al.) centered at 104.8 cm^{-1} (95.4 μm). As said before, any of the band peaks observed in NGC 7027 around $\sim$98 μm ($\sim$102 cm^{-1}) could well be responsible of the ν_7 mode. However, only the best fit to the band including the C_6 model is shown in Fig. 1. If the carrier of the 95.5 μm feature is finally C_5 at ν_7=104.8 cm^{-1}, the estimated column density assuming an excitation temperature of 100 K (typical of a PNe envelope) is $N(C_5)$=1.8$\times$10^{14} cm^{-2}. Assuming 1.5–4.0 magnitudes of visual extinction in the neutral envelope (Hasegawa et al. 2000), the typical abundance of C_5 in NGC 7027 would be (0.5–1.0)$\times$10^{-7}, similar to that derived by Bernath et al. (1989) in IRC+10216.

Fig. 2 shows that, for the same column densities required to reproduce the bending modes, the ν_4 and ν_3 stretching modes of C_6 and C_5 are not detected in NGC 7027. Different excitation conditions of the stretching and bending modes and geometrical effects may explain this conjecture. Although carbon clusters have a moderate size, we could also expect an efficient pumping of the stretching and bending modes through UV photons. Mid–IR photons could also contribute to the excitation of the high–$\nu_{bending}$ excited states but also of the stretching modes. Finally, the low–energy bending modes could be pumped alone by the absorption of far–IR dust photons (see the case of the C_3 excitation in Cernicharo et al. 2000). However, the smaller volume of the photon–dominated regions relative to the far–IR dusty envelope in NGC 7027, and the larger mid–IR flux of IRC+10216 (where the C_3 and C_5 stretching modes were detected) compared to NGC 7027 (a factor $\sim$10^3 at 5 μm, but only a factor $\sim$4 at 100 μm), can favor the observation of the C_n bending modes within the large ISO beam. Under these conditions, the detection of the bending modes and the non–detection of the stretching modes in NGC 7027 can be plausible.

The ν_9 low–energy bending mode of C_6 is even less known. *Ab inito* calculations predict a $\nu_9\sim$108 cm^{-1} frequency and an infrared intensity of $\sim$25 km mol^{-1} [$A(\nu_9 = 1-0)\simeq$0.035 s^{-1}; Martin et al. 1990; 1995), while photoelectron spectroscopy experiments estimate ν_9=97$\pm$45 cm^{-1} (Arnold et al. 1991) and ν_9=90$\pm$50 cm^{-1} (Xu et al. 1997). Theo-

retical predictions have to be taken into account with caution since they rely in the harmonic approximation which can be in error for large amplitude benders such as radicals with low-lying electronic states. In particular, the infrared intensity has to be considered as a lower limit (and column densities as upper limits). *Ab initio* calculations do predict a low-lying electronic state for open–shell species such as C_4 or C_6. The term value for the $^1\Delta_g$ lowest energy excited state of C_6 has been recently determined by Xu et al. only at $\sim$1400 cm^{-1} from the ground. Hence, A_{SO} can effectively be large even in the ground state (Λ=0). As an example, the A_{SO} constant of C_4H ($^2\Sigma$ ground state) is very large, $\simeq$3 cm^{-1} (Yamamoto et al. 1987), because its $^2\Pi$ electronic excited state is only $\simeq$468 cm^{-1} above the ground. In the case of even–numbered C_n chains, A_{SO} can easily be larger because of the higher spin multiplicity of the ground state and the larger Λ value of the lowest–lying electronic excited state. Fig. 1 also shows the expected band–shape for a $^3\Pi_{vib} - {}^3\Sigma_{vib}$ transition with A_{SO}=3.5 cm^{-1} (we estimated $A_{SO}\sim$4 cm^{-1} for C_4), C_6 molecular constants from Hwang et al. (1993) and van Zee et al. (1987;1988), and the ν_9 band origin at 98.3 cm^{-1} (101.7 μm). Assuming the same excitation temperature than for C_5 we derive $N(C_6)=0.8\times10^{14}$ cm^{-2}. Hence, the C_6 abundance will be a factor 2 smaller than that of C_5.

Much more work has to be done to fully understand and characterize the low–energy vibrations of C_n chains in order to assign the UfIBs observed by ISO. The cyclic C_n isomers could also produce spectral features in the far–IR, however, their active modes are even less known. Waiting for such progresses, space observations offer the unique opportunity to obtain spectra in the far–IR domain where the bending modes appear and to motivate further laboratory and theoretical studies. The presence of small C_n chains in the space as well as their high reactivity, suggest that these species can be involved in the formation of more complex organic molecules. In fact, for cumulenic clusters with n=10 to 20, linear structures are thought to close into rings, while for n>30, these species are thought to be more stable in aromatic and fullerene–like structures (O' Brien et al. 1987).

Future space heterodyne telescopes, such as the *Herschel Space Observatory*, with much better sensitivity and spectral resolution in the far–IR, should allow the detection of longer C_n chains through their low–energy bending modes. This will be the fingerprint needed to understand the formation and the nature of the UIBs and UfIBs carriers.

We thank Spanish DGES and PNIE for funding support under grants PANAYA2000-1784, ESP2001-4516, AYA2002-10113-E, ESP2002-01627, AYA2002–02117 and AYA2003-02785-E. We also thank Ana Heras for providing us the processed SWS spectrum of NGC 7027 and F. Najarro and C. Joblin for useful comments about atomic lines and PAHs respectively. We have used the Atomic Line List v2.04 of Peter van Hoof (http://www.pa.uky.edu/~peter/atomic).

REFERENCES

Arnold, D. W., Bradforth, S. E., Kitsopoulos, T. N. & Neumark, D. M. 1991, JChPh, 95, 8753

Avery, L. W., Broten, N. W., MacLeod, J. M., Oka, T., & Kroto, H. W. 1976, ApJ, 205, L173

Bachiller, R., Forveille, T., Huggins, P. J., & Cox, P. 1997, A&A, 324, 1123

Baluteau, J.-P., Zavagno, A., Morisset, C., & Pequignot, D. 1995, A&A, 303, 175

Bell, M. B., Feldman, P. A., Travers, M.J., McCarthy, M.C., Gottieb, C.A. & Thaddeus, P. 1997, ApJ, 483, L61

Bernard Salas, J., Pottasch, S. R., Beintema, D. A., & Wesselius, P. R. 2001, A&A, 367, 949

Bernath, P.F., Hinkle, K.H., & Keady, J.J. 1989, Science, 244, 562

Broten, N. W., Oka, T., Avery, L. W., MacLeod, J. M., & Kroto, H. W. 1978, ApJ, 223, L105

Cernicharo, J., Kahane, C., Gómez-González, J., & Guélin, M. 1986, A&A, 164, L1

Cernicharo, J. & Guélin, M. 1996, A&A, 309, L27

Cernicharo, J., Barlow, M. J., Gonzalez-Alfonso, E. et al. 1996, A&A, 315, L201

Cernicharo, J., Liu, X.W., González-Alfonso, E., Cox, P., Barlow, M. J., Lim, T., Swinyard, B. M. 1997, ApJ, 483, L65

Cernicharo, J., Goicoechea, J.R., & Caux, E. 2000, ApJ, 534, L199

Cernicharo, J., Heras, A.M., Tielens, A. G. G. M., Pardo, J.R., Herpin, F. Guelin, M., Waters, L. B. F. M. 2001, ApJ, 546, L123

Cernicharo, J., Goicoechea, J.R., & Benilan, Y. 2002, ApJ, 580, L157

Cernicharo, J. 2004, ApJ, in press.

Clegg, P. E., et al. 1996, A&A, 315 L38

de Graauw, T., et al. 1996, A&A, 315, L49

Douglas, A.E. 1977, Nature, 269, 130

Giesen, T. F., Berndt, U., Yamada, K.M.T. et al. 2001b, ChemPhysChem. 4, 242

Gillett, F. C., Forrest, W. J., & Merrill, K. M. 1973, ApJ, 183, 87

Guélin, M., Cernicharo, J., Kahane, C., Gómez-González, J., & Walmsley, C. M. 1987, A&A, 175, L5

Guélin, M., et al. 1997, A&A, 317, L1

Hasegawa, T., Volk, K., & Kwok, S. 2000, ApJ, 532, 994

Heath, J. R., Cooksy, A. L., Gruebele, M. H. W., Schmuttenmaer, C. A., & Saykally, R. J. 1989, Science, 244, 564

Herpin, F., Goicoechea, J. R., Pardo, J. R., & Cernicharo, J. 2002, ApJ, 577, 961

Hinkle, K.W., Keady, J.J., & Bernath, P.F. 1988, Science, 241, 1319

Hutter, J., & Lüthi, H.P., 1994, JChPh, 101, 2213

Hwang, H.J., van Orden, A., Tanaka, K., Kuo, E.W., Heath, J.R., & Saykally, R. J. 1993, JMolPhys, 79, 769

Kessler, M. F., Steinz, J. A., Anderegg, M. E. et al. 1996, A&A, 315, L27

Kitsopoulos, T. N., Chick, C. J., Zhao, Y., & Neumark, D. M. 1991, JChPh, 95, 5479

Kroto, H. W., Kirby, C., Walton, D. R. M., Avery, L. W., Broten, N. W., MacLeod, J. M., & Oka, T. 1978, ApJ, 219, L133

Latter, W.B., Dayal, A., Bieging, J.H., Meakin, C,, Hora, J.L., Kelly, D.M. & Tielens, A. G. G. M. 2000, ApJ, 539, L783

Martin, J.M.L, Francois, J.P., & Gijbels, R. 1990, JChPh, 93, 8850

Martin, J.M.L, El–Yazal, J., & Francois, J.P. 1995, ChemPhysLett, 242, 570

Masson, C.R. et al. 1985, ApJ, 292, 464

Moazzen-Ahmadi, N., McKellar, A. R. W., & Amano, T. 1989, JChPh, 91, 2140

O'Brien, S.C., Heath, J.R., Curl, R.F., & Smalley, R.E. 1987 JChPh, 88, 220

Swinyard, B. M., et al. 1996, A&A, 315, L43

Turner, B. E. 1971, ApJ, 163, L35

van Orden, A., & Saykally, R.J. 1998, ChemRev, 98, 2313–2357

van Zee, R. J., Ferrante, R. F., Zeringue, K. J., & Weltner, W., Jr. 1987, JChPh, 86, 5212

van Zee, R. J., Ferrante, R. F., Zeringue, K. J., Weltner, W., Jr., & Ewing, D. W. 1988, JChPh, 88, 3465

Volk, K., & Kwok, S. 1997, ApJ, 477, 722

Xu, C., Burton, G.R., Taylor, T.R., & Neumark, D.M. 1997, JChPh, 107, 3428

Yamamoto, S., Saito, S., Guelin, M., Cernicharo, J., Suzuki, H., & Ohishi, M. 1987, ApJ, 323, L149

Zhang, K., Guo, B., Colarusso P. & Bernath, P.F. 1996, Sci, 274, 582

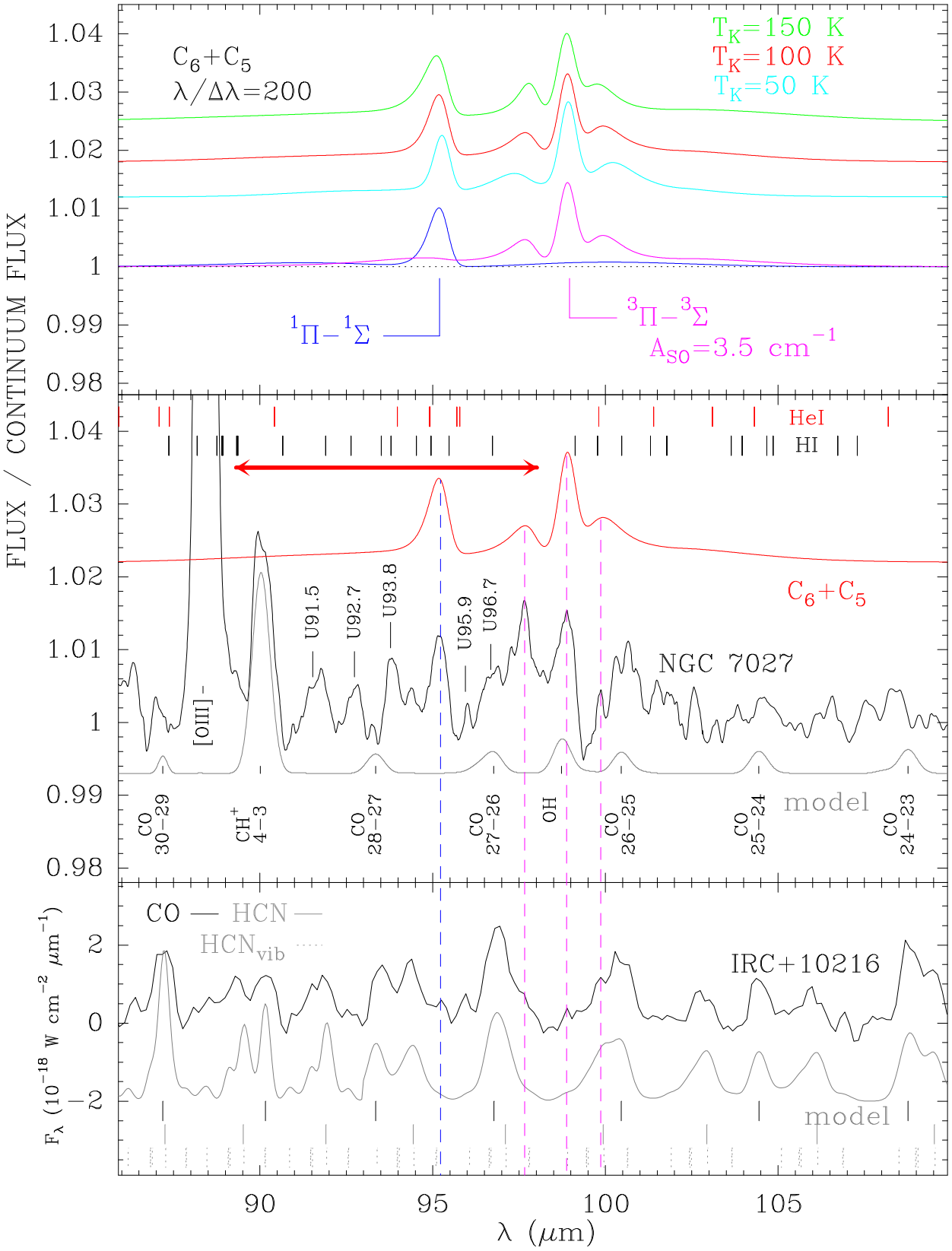
C6+C5
λ/Δλ=200
TK=150 K
TK=100 K
TK=50 K
1Π−1Σ
3Π−3Σ
ASO=3.5 cm−1
FLUX / CONTINUUM FLUX
HeI
HI
C6+C5
NGC 7027
[OIII]
U91.5
U92.7
U93.8
U95.9
U96.7
CO 30−29
CH+ 4−3
CO 28−27
CO 27−26
OH
CO 26−25
CO 25−24
CO 24−23
model
CO — HCN —
HCNvib
IRC+10216
model
Fλ (10−18 W cm−2 μm−1)
λ (μm)

Fig. 1.— *Top panel*: Expected band shape for a $^1\Pi_{vib} - {}^1\Sigma_{vib}$ transition (as the ν_7 mode of C_5) and for a $^3\Pi_{vib} - {}^3\Sigma_{vib}$ transition (as the ν_9 mode of C_6) with A_{SO}=3.5 cm^{-1}. The excitation temperature for both transitions is 100 K. The intrinsic line width is 10 km s^{-1} and the spectral resolution $\lambda/\Delta\lambda$ is 200. —*Middle panel*: Observed ISO/LWS spectrum of NGC 7027 between ∼86 and 110 μm. The ordinate corresponds to the flux over the continuum flux and the abscissa to the wavelength in μm. Large Velocity Gradient model for the pure rotational emission of CO, CH^+ and OH (Herpin et al. 2002) and the total model for the bending modes of C_5 and C_6. The thick horizontal arrow represents the observational uncertainty for the ν_7 C_5 band origin (from Kitsopoulos et al. 1991). The experimental uncertainty for the ν_9 C_6 mode is 90±50 cm^{-1} (Xu et al. 1997). See text. — *Bottom panel*: Observed ISO/LWS spectrum of IRC+10216 between ∼86 and 110 μm. The ordinate corresponds to the continuum subtracted flux and the abscissa to the wavelength in μm. Large Velocity Gradient model for the pure rotational emission of CO ν=0, 1, ^{13}CO ν=0, HCN and H^{13}CN ν =0, and HCN_{vib} ν_2=1, 2 and $\nu_{1,3}$=1 (Cernicharo et al. 1996). The rotational transitions of CO, HCN in the ground state, and HCN_{vib} ν_2=1, 2 and $\nu_{1,3}$=1 are indicated.

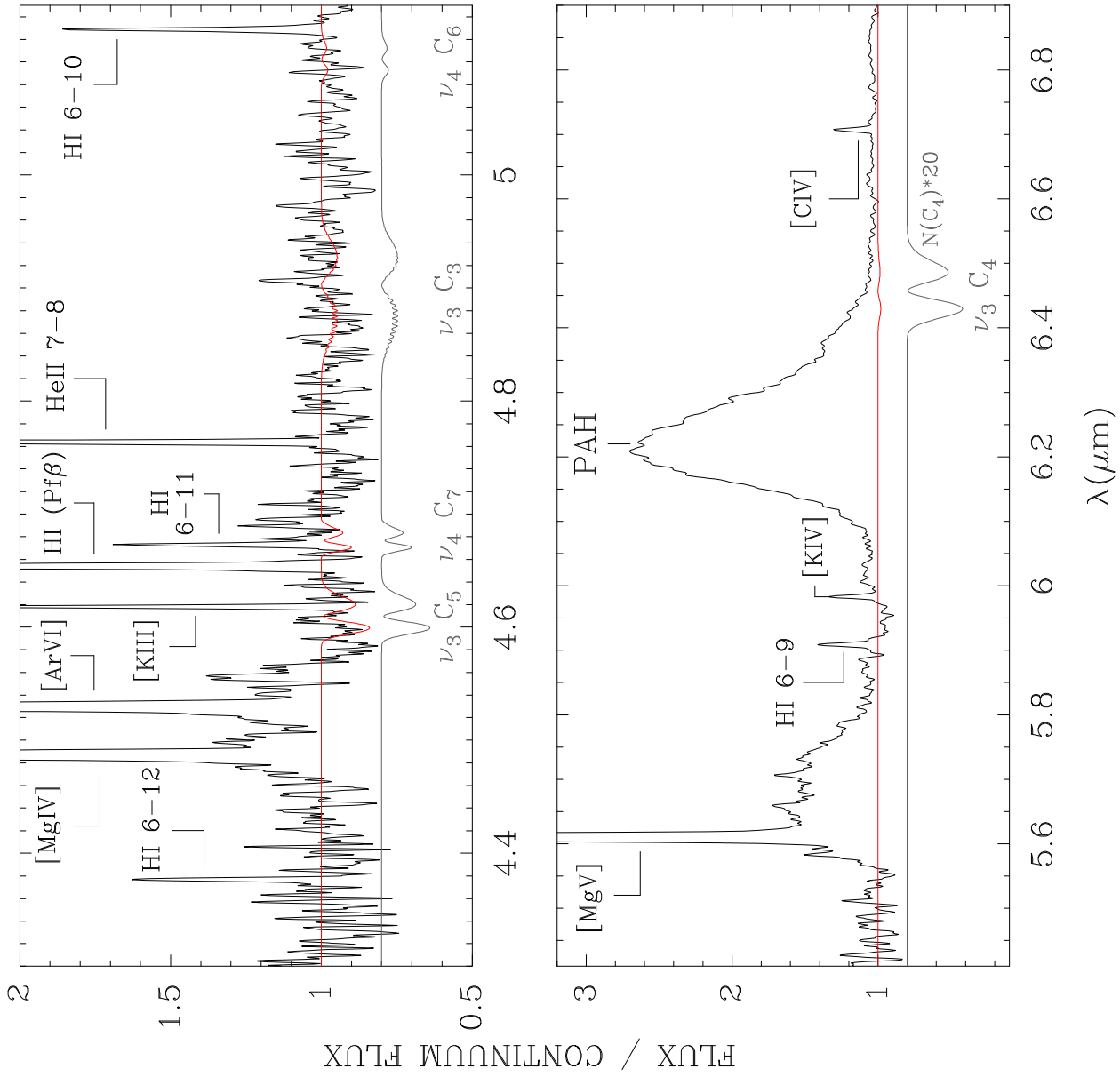

Fig. 2.— Observed ISO/SWS spectrum of NGC 7027 between ∼4 and 7 μm. The ordinate scale is F/F$_c$ and the wavelength is in μm. The fine structure and recombination lines from the ionized region are labeled. The expected $\Sigma_{vib} - \Sigma_{vib}$ parallel spectra from the ν_3 C$_3$, ν_3 C$_4$, ν_3 C$_5$, ν_4 C$_6$ and ν_4 C$_7$ stretching modes are also shown. The excitation temperature for all bands is also 100 K. The intrinsic line width is 10 km s^{-1} and the spectral resolution $\lambda/\Delta\lambda$ is 1500. Column densities are N(C$_5$)=1.8×10^{14} cm^{-2} (from the ν_7 bending mode), N(C$_6$)=0.8×10^{14} cm^{-2} (from the ν_9 bending mode), N(C$_3$)=10×N(C$_5$), N(C$_7$)=N(C$_5$)/10 and N(C$_4$)=0.8×10^{15} cm^{-2} (from Cernicharo et al. 2002).